TECHNICAL REPORT NO. 320

Implicit Functions for Modeling Arbitrary Deformable Shapes

by

Andrew J. Hanson

November 1990

COMPUTER SCIENCE DEPARTMENT
INDIANA UNIVERSITY
Bloomington, Indiana 47405-4101

Implicit Functions for Modeling Arbitrary Deformable Shapes *

Andrew J. Hanson

Department of Computer Science
Indiana University
Bloomington, Indiana 47405

Abstract

We introduce a new implicit-function approach to shape modeling. The method uses a generalized L_p norm to construct convex, non-convex, and disconnected shapes whose asymptotic forms as $p \to \infty$ are boolean *and* and *or* combinations of shape primitives. Linear primitives produce shapes of the superquadric family that approach polyhedral bounds as $p \to \infty$ and ellipsoids as $p \to 2$. While the approach is distinct from Blinn's blobby model method, it has the following characteristics in common with blobby models: (1) solutions of the implicit function equation must be computed numerically in all but a few special cases; (2) there are no seams or artifacts where primitives are combined; (3) once a given point on the surface is known, surface normals and curvatures for shading and tesselation operations can be computed analytically at that point.

*This research was supported in part by National Science Foundation Grant No. IST-8511751, and in part by Defense Advanced Research Projects Agency Contract No. MDA903-86-C-0084.

1 Introduction

We introduce a new implicit-function approach to shape-modeling that uses a generalized L_p norm to construct boolean combinations of shape primitives. The resulting models include nonconvex and disconnected shapes, and possess natural classes of smooth deformations.

Linear functions are particularly useful shape primitives because they produce shapes that smoothly approach arbitrary polyhedra as $p \to \infty$. Convex shapes of the superquadric family [2,3,8,6] are a special case of such models that become ellipsoids as $p \to 2$. We suggest a new class of linear shape primitives whose asymptotes are planar-bounded half-spaces.

Implicit-function shape models such as our L_p norm model and Blinn's blobby model approach [4] share the following desirable features:

- **A global equation with local parts.** The entire model is described by a single implicit equation that may nevertheless have localizable parts that simplify some types of analysis. Solutions of the implicit-function equation must be computed numerically in all but a few special cases. Since the equation is interpretable as a density function whose level sets define the surface model, explicit tesselations can be constructed using the weaving wall or marching cube techniques [1,7].

- **Analytic normals and curvatures.** Once a given point on the surface is known, surface normals and curvatures for ray-traced shading, faceted shading and curvature-based tesselation operations can be computed analytically at that point. There are no seams or artifacts in the surface normals where primitives are combined.

The remainder of the paper is organized as follows: In Section 2, we define a generalized L_p norm that combines primitive shapes with boolean *and* and *or* operations, thus permitting the unified treatment of concave, convex, and disconnected shapes. In Section 3, we examine some useful primitive functions, emphasizing those producing shapes that deform smoothly inward from exterior polyhedral bounds. Finally, we give some examples of shapes modeled using these techniques.

2 Shape from Generalized L_p Norms

The L_p norm in 2, 3, or D dimensions is defined as

$$\begin{aligned} \| x, y \|_p &= (|x|^p + |y|^p)^{1/p} \\ \| x, y, z \|_p &= (|x|^p + |y|^p + |z|^p)^{1/p} \\ \| \vec{x} \|_p &= \left(\sum_{i=1}^{D} |x_i|^p \right)^{1/p} . \end{aligned} \tag{1}$$

Equation (1) can be understood as an interpolation function relating the following classical metrics:[1]

- **City Block.** For $p = 1$, we have a "city block" or Manhattan metric that gives the distance between two points as the sum of their cartesian coordinate differences. The level sets of this metric are diamonds, octahedra, and so on.
- **Euclidean.** For $p = 2$, we have the standard Euclidean distance, which is the square root of a quadratic form invariant under orthonormal spatial rotations. The level sets are spheres.
- **Chessboard.** In the limit $p \to \infty$, the distance function is the maximum of the values of the cartesian coordinates, so that the level sets of the metric correspond in 2 dimensions to concentric squares like the pattern on a chessboard. In higher dimensions, the level sets are cubes and hypercubes.

We now present our generalization of Eq. (1) that can be exploited to produce implicit functions for arbitrary shape classes, followed by a discussion justifying the form chosen.

2.1 The Fundamental Implicit Function Equation

We propose the following generalization of the L_p norm as a fundamental implicit function equation for modeling shapes that are built from boolean combinations of differentiable elementary shape primitives $\{H_i(\vec{x})\}$:

$$F(\vec{x}) = \left(\sum_{\{and's\}} \frac{1}{\sum_{\{or's\}} \left| \frac{1}{H_i(\vec{x})} \right|^p} \right)^{1/p} = w. \qquad (2)$$

The variable w on the right-hand-side can be thought of as a distance from an origin or as the radius of a generalized sphere; while we will usually set w to unity, it is sometimes useful to observe the evolution of the shape equation as a function of w. Depending upon the primitives being used, one may wish to impose the condition $p > 1$, since corners, cusps and other singular nonconvex phenomena may occur for $p \leq 1$.

We note that the *and* operation has the form of the addition law for series resistors, while the *or* operation has the form of the addition law for parallel resistors, making the entire equation similar in form to the description of an arbitrary network of resistors. The shape can thus be represented as a graph isomorphic to the corresponding network of resistors, as illustrated in Figure 1.

[1]The L_p norm is also commonly known as a *Minkowski metric* (see, e.g., [9]), but should not be confused with metrics that are locally invariant under Lorentz transformations on a negative signature Minkowski space.

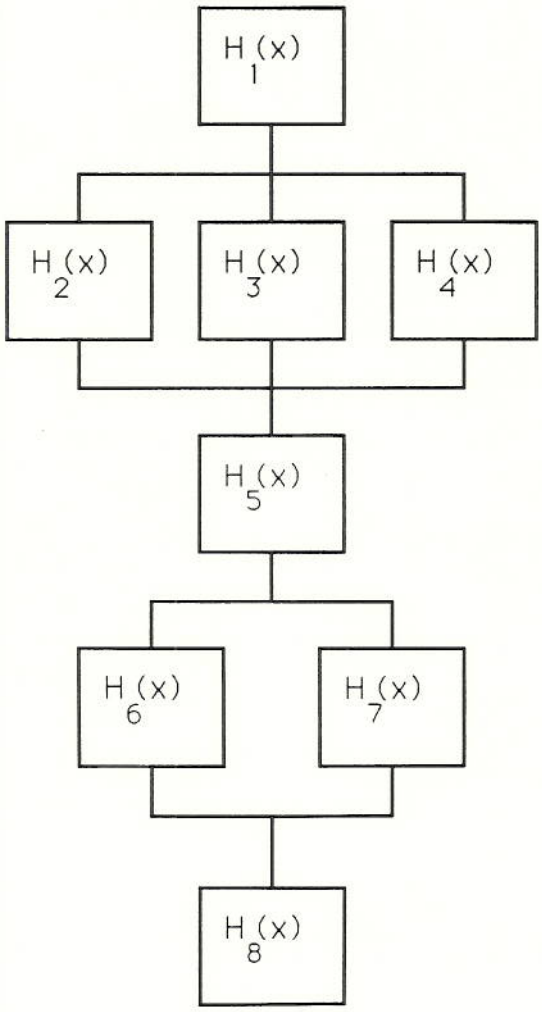

Figure 1: An example of a graphical representation of a shape composed of the *and* of the primitives H_1, H_5, H_8 with the *or* of H_2, H_3, H_4 and the *or* of H_6, H_7.

If desired, the general form (2) may be easily generalized to include hyperbolic spaces, terms with unequal exponents, and arbitrary dimensionality of $\vec{x}$.

Our use of the boolean terminology (*and* and *or*) in Eq. (2) refers, strictly speaking, to the *asymptotic form* of the equation in the limit $p \to \infty$. In this limit, the equation can be written as

$$F(\vec{x}) = \max_{\{and's\}} \left(\min_{\{or's\}} \left(H_{a_1}(\vec{x}), H_{a_2}(\vec{x}), \ldots\right), \min_{\{or's\}} \left(H_{b_1}(\vec{x}), H_{b_2}(\vec{x}), \ldots\right), \ldots \right) = w. \tag{3}$$

Using the algebraic *max* operation combined with the *min* operation on sets of primitives produces functions whose bounding level sets are all possible shapes that can be generated from boolean *and* and *or* operations on those primitives.

Each primitive $H_i(\vec{x})$ in turn dominates the asymptotic shape for the portion of the surface (if any) where it is the solution of Eq. (3); in other words, the i-th asymptotic portion of the surface obeys the equation

$$|H_i(\vec{x})| = w, \tag{4}$$

or, when $H_i(\vec{x})$ can be both positive and negative, one of the pair of equations

$$H_i(\vec{x}) = \pm w. \tag{5}$$

Planar asymptotes result either when $H_i(\vec{x})$ is explicitly linear in $\vec{x}$, or when Eq. (5) reduces after algebraic manipulation to one that is linear in $\vec{x}$.

2.2 Convex polygons from an L_p norm with positive powers

If the *or* terms consist of single components, Eq. (2) reduces to a shape equation of the hyperquadric form [6], which includes superquadrics as a special case:

$$F(\vec{x}) = \left(\sum_{\{and's\}} |H_i(\vec{x})|^p \right)^{1/p} = w. \tag{6}$$

We can view this case of the shape equation as a standard L_p norm, Eq. (1). If we take $\vec{x}$ to be a D-dimensional vector, set $w = 1$, and let $i = 1, \ldots, N$, the asymptotic outer limit of the shape defined by the implicit function $F(\vec{x}) = 1$ is the logical *and* of all the regions in D-space solving Eq. (5); the asymptotic form is simply a special case of Eq. (3):

$$F(\vec{x}) = \max\left(|H_1(\vec{x})|, |H_2(\vec{x})|, \ldots, |H_N(\vec{x})|\right) \quad . \tag{7}$$

When the primitives are taken to be the linear functions,

$$H_i(\vec{x}) = \left(\vec{n}_i \cdot \vec{x} + d_i\right), \tag{8}$$

where the $\vec{n}_i$ are vectors in D dimensions and the d_i are a set of N constants[6], Eq. (5) then describes a family of *strips* whose logical *and* produces *arbitrary convex polytopes.*

In Figure 2, we use the primitive $H(\vec{x}) = n_x x + n_y y + d = \pm 1$ to construct assorted 2-dimensional shapes with asymptotic polygonal bounds. As p varies in the range $\infty > p \geq 2$, Figure 2(b) and (c) will deform smoothly inward from their indicated convex polygonal bounds to ellipsoids.

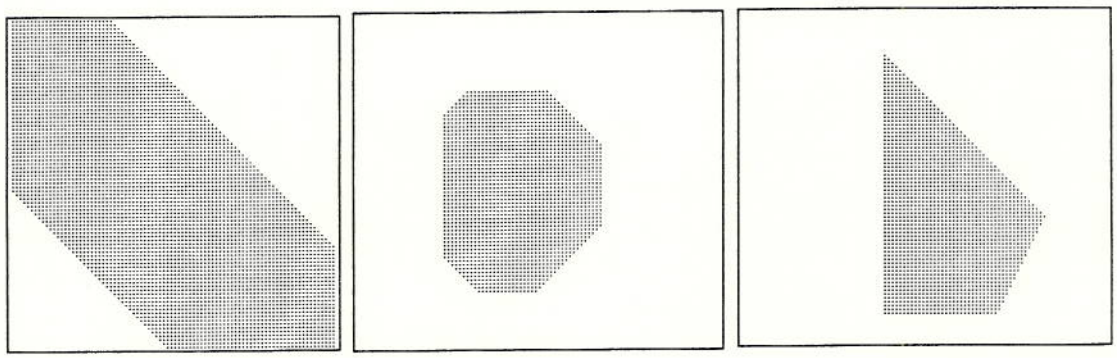

Figure 2: (a) A single isolated shape primitive: the strip bounded by $|n_x x + n_y y + d| \leq 1$. (b) Taking the intersections of four such strips to form a convex polygon. (c) Constructing a polygon whose faces do not have matching parallel faces by taking one side of each strip to lie outside the body of the shape.

2.3 Nonconvex polygons from negative powers

Next, we show how the form chosen in Eq. (2) can be used to model *nonconvex* shapes with controllable deformations.

The fundamental operation required to obtain nonconvex limits from convex primitives is the logical *or* operation, as shown in Figure 3. This operation can equivalently be performed by computing the logical complement of the intersection of the complements of the shape primitives. Thus, all we need is a way to get the logical complement of a shape primitive; we can achieve that in the framework of an L_p norm by using *negative powers* in the norm.

To give an intuitive feeling for this construction, we first observe that the algebraic *minimum* function,

$$F(\vec{x}) = \min\left(|H_1(\vec{x})|, |H_2(\vec{x})|, \ldots, |H_N(\vec{x})|\right) = w, \tag{9}$$

produces bounding level sets that *or* together all the primitive shapes, as we require. Our goal is then to achieve an analytic form whose limit is the *minimum* function.

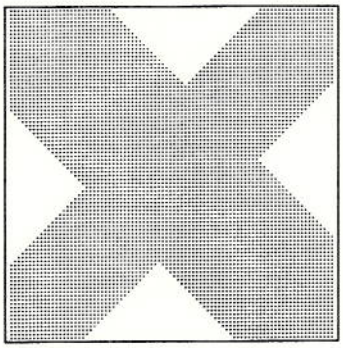

Figure 3: The elementary forms needed for *nonconvex* polygons can be made using the logical *or* of geometric strips.

We begin by noting that the "inside" of a shape is transformed to its "outside" by taking the inverse, i.e., $|x|^p \rightarrow |x|^{-p}$. Figure 4 plots this function for several positive and negative values of p to show how the "interior" of $|x|^p < 1$ switches domains as p passes through zero. Using this form of the logical complement by itself is not completely satisfactory, since singularities can occur at the origin. However, if we sum the desired terms to produce the intersection of the complements, possibly singular at various places, we can remove the singularities by inverting again; this inversion achieves the rest of the desired result by mapping the intersection of the complemented primitives to its own complement, thereby yielding a net logical *or* operation. We illustrate this process in Figure 5, and represent it in our framework by expressions of the form

$$F(\vec{x}) = \left(\frac{1}{\sum_{i=1}^{N} \left| \frac{1}{H_i(\vec{x})} \right|^p} \right)^{1/p} = w. \tag{10}$$

The bounding level sets of Eq. (10) as $p \rightarrow \infty$ are given by Eq. (9), so this equation explicitly realizes our objective. Numerical computations can handle the singularities that may occur by using such techniques as rationalizing the fractions in Eq. (10) or adding small positive constants to $H_i(\vec{x})$; analytically, the implicit function is not actually singular unless the chosen primitive functions are pathological.

3 Primitives

We may choose the primitive functions $H_i(\vec{x})$ that make up the terms in the shape functions to have properties appropriate to particular modeling tasks. Any differentiable function can in principle be used, but some have more interesting consequences than others.

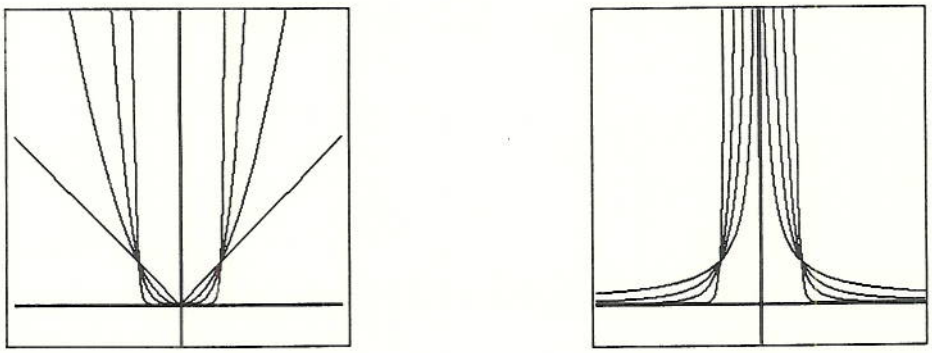

(a) (b)

Figure 4: The primitive function $|x|^p = w$; the horizontal axis is x and the vertical axis w. (a) Positive powers (1.0, 2.0, 4.0 and 16.0), showing the approach to a square well for large powers. the "interior," $|x|^p =\leq 1$, is the interval $-1 \leq x \leq +1$. (b) Negative powers (-1.0, -2.0, -4.0 and -16.0), showing the approach to a square pillar for large negative powers. The "interior" excludes $-1 < x < +1$.

Double-Faced Primitives. We have already seen in Figures 2 and 3 examples of strictly linear primitives of the form:

$$|H_i(\vec{x})| = |\vec{n}_i \cdot \vec{x} + d_i| = w \quad \rightarrow \quad \vec{n}_i \cdot \vec{x} = -d_i \pm w = c_i^{\pm}. \tag{11}$$

where $\vec{n}_i$ is any vector. The solutions produce pairs of parallel planar asymptotes.

Whatever vector is chosen, the parallel pair of surfaces corresponding to *both sides* of Eq. (11) will occur as delimiters. Suppose we now want to describe a shape that is *not symmetric*, and thus has a limiting face with no corresponding parallel face. One way to accomplish this is to choose d_i and $\vec{n}_i$ so that the second face is outside the limits of the figure determined by other primitives, as was done in Figure 2(c).

This double-sidedness of linear primitives may be understood by considering them as limiting cases of elliptical primitives of the form

$$H(\vec{x}) = \left\{ \left(\frac{x}{a}\right)^2 + \left(\frac{y}{b}\right)^2 \right\}^{(1/2)} \overset{b \to \infty}{\longrightarrow} \left|\frac{x}{a}\right|, \tag{12}$$

where x can of course be replaced by $(\vec{n} \cdot \vec{x} + d)$ in general.

The existence of hidden partners for double-sided primitives is not a serious problem, since the hidden faces can always be placed far enough away that their effect on the shape deformation is negligible. However, this phenomenon is aesthetically displeasing, and introduces superfluous behavior into the description. We next describe some alternative primitives without hidden parallel partners.

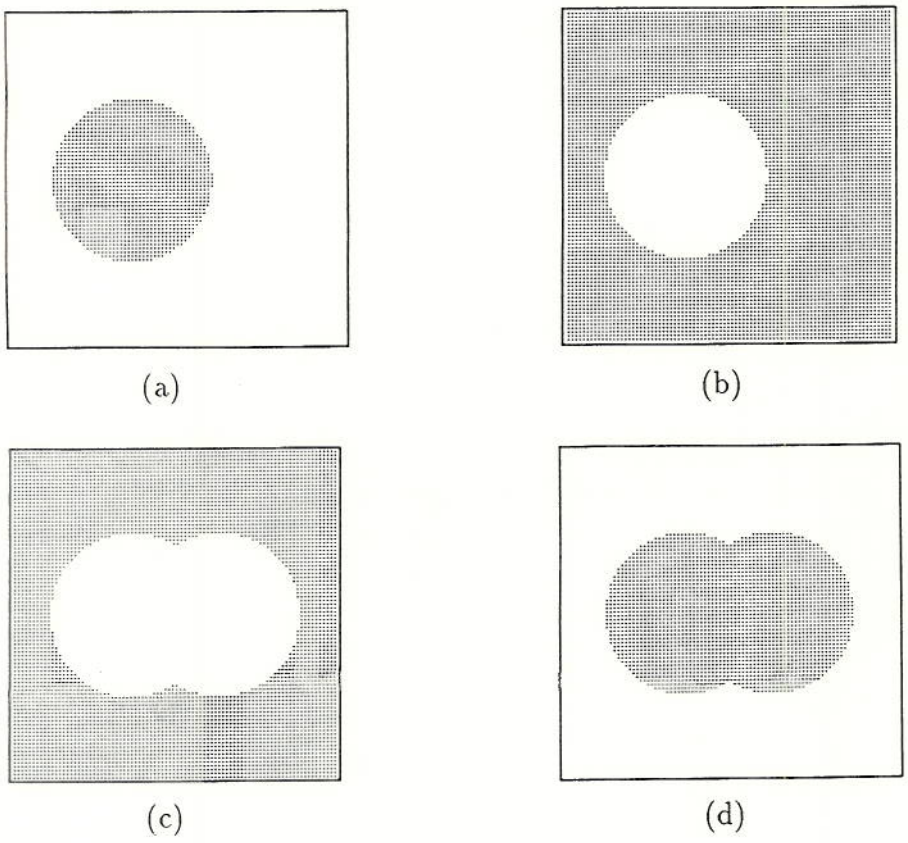

Figure 5: Performing an *or* operation algebraically. (a) One of a pair of circles. (b) The complement of the circle found by inverting its equation. (c) The intersection of the complements of two slightly displaced circles. (d) The final result obtained by inverting the intersection of the complements.

Single-Faced Planar Primitives. If we want to describe shapes with planar-faced limits in the most elegant possible manner, we require primitives that, rather than being less than unity within a band or slab, are less then one for an *entire half-space*. One may consider such primitives to be related to the linear primitives by a transformation that takes the elliptical approximation (12) and maps a point on the hidden-partner face to ∞, resulting in straight line from some finite point through ∞. We now examine some useful classes of such primitives.

The boundary of a half-space in any dimension is the equation of a plane,

$$h(\vec{x}) = \frac{\vec{n} \cdot \vec{x}}{c} \tag{13}$$

$$= 1 \ . \tag{14}$$

Here $\vec{n}$ is the normal to the plane and c is the distance from the origin to the plane.

A general form of the equation for a single-faced planar primitive is constructed from the primitive equation $h(\vec{x}) = w$ by performing two transformations: First, we apply a function $f(p)$ to the primitive equation,

$$f(h(\vec{x})) = f(w), \tag{15}$$

and then we add another arbitrary analytic function $g(\vec{x})$ to both sides of the equation, dividing by the right hand side to achieve

$$\frac{f(h(\vec{x})) + g(\vec{x})}{f(w) + g(\vec{x})} = 1. \tag{16}$$

The particular choice of transformation functions f and g depends upon the modeling goals. Examples include

$$H(\vec{x}) = \frac{2}{1 + \exp(-(\frac{\vec{n} \cdot \vec{x}}{c} - 1))} \tag{17}$$

$$H(\vec{x}) = \frac{\left|\frac{\vec{n} \cdot \vec{x}}{c}\right|}{1 - \frac{\vec{n} \cdot \vec{x}}{c} + \left|\frac{\vec{n} \cdot \vec{x}}{c}\right|}. \tag{18}$$

The particular form that we prefer is a ratio of quadratic forms,

$$\begin{aligned} H(\vec{x}) &= \frac{\left|\frac{\vec{x}-\vec{a}}{2c}\right|^2}{\left|\frac{\vec{x}-\vec{a}}{2c} - \vec{n}\right|^2} \\ &= \frac{\left|\frac{\vec{x}-\vec{a}}{2c}\right|^2}{1 - \frac{\vec{n} \cdot \vec{x}}{c} + \left|\frac{\vec{x}-\vec{a}}{2c}\right|^2} \\ &= \frac{-1 + \frac{\vec{n} \cdot \vec{x}}{c} + \left|\frac{\vec{x}-\vec{a}}{2c} - \vec{n}\right|^2}{\left|\frac{\vec{x}-\vec{a}}{2c} - \vec{n}\right|^2}. \end{aligned} \tag{19}$$

Such a ratio is interpretable as the result of using a conformal transformation,[2]

$$\vec{x}' = \frac{\vec{x} - \vec{q}|\vec{x}|^2}{1 - 2\vec{q}\cdot\vec{x} + |\vec{q}|^2|\vec{x}|^2} \quad , \tag{20}$$

to map the equation of a circle to the straight line Eq. (14). The function Eq. (19) has one isolated zero and one isolated pole, which are interchanged when we use the inverse of the primitive function in an *or* term of the shape equation. These singularities are easily sidestepped by standard techniques such as moving the pole off into the complex plane by adding a small constant term to both numerator and denominator, e.g., $(x)^2 \rightarrow (x^2 + \epsilon^2)$ where ϵ is a small number. In Figure 6, we plot this nonsingular modification of Eq. (19) as a function of w.

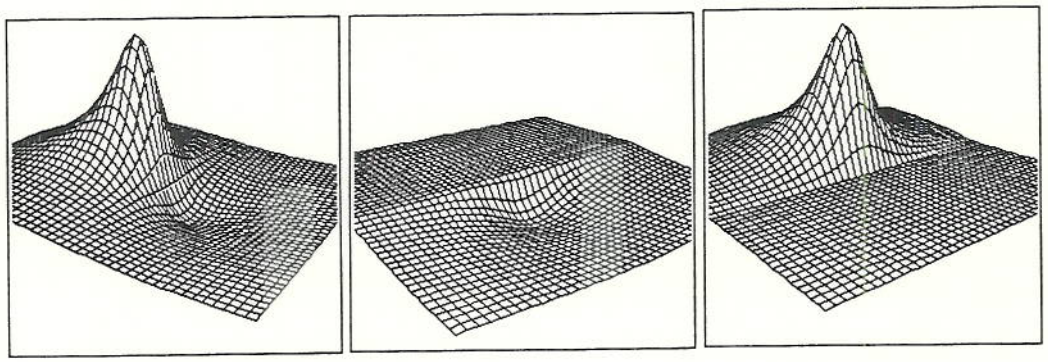

(a) (b) (c)

Figure 6: Equation (19), a ratio of two circles that reduces to a linear function, represented in w-space as a function on an (x, y) grid. (a) The bare function; (b) the function truncated above $w = 1$ to show the straight line; (c) truncated below $w = 1$. This function has one isolated zero and one isolated pole that are displaced from the real plane by adding a small constant to both numerator and denominator.

Nonlinear Primitives: Instead of using primitives that reduce to the linear equation (14) to describe the asymptotic bounds in shape space, we could also use any equation whatever; for example, if we replaced equations of planes with equations of spheres, we would produce shapes whose limiting boundaries for large exponents

[2]Equation (19) is the analog in D Euclidean dimensions of the complex linear fractional transformation

$$z' = z/(1 + \alpha z) \, ,$$

which reduces to Eq. (19) with $\mathrm{Re}(\alpha) = q_1, \mathrm{Im}(\alpha) = -q_2$ for $D = 2$, and is well known to transform circles conformally into lines and vice-versa.

were intersections and unions of collections of spheres, rather than intersections of planar-bounded spaces. If we had a particular application in which the deformations required more complex limits, we could recursively insert *any shape model we wish* in place of the elementary primitives.

As an example of a more complex primitive, we show in Figure 7 a two-dimensional ring,

$$(x^2 + y^2 - r^2)^2 - R^2 = w$$

as a function of w. Variants of such equations in three dimensions produce tori and hollow spheres, but are of course impossible to plot in terms of the fourth dimension w.

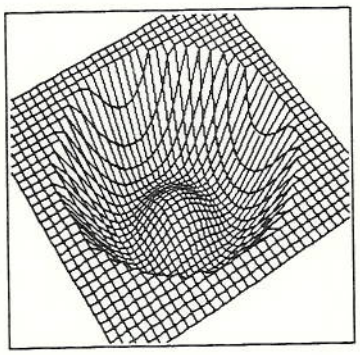

Figure 7: The primitive $(x^2 + y^2 - r^2)^2 - R^2 = w$ plotted as a function of w and truncated at $w = 10$. Slicing through the primitive at $w = 1$ gives the equation of a 2-dimensional ring.

Comparison to Blobby Models: Blinn's "blobby" models [4] are an alternative approach to achieving many of the results we have sought in this paper. In reference [6], we in fact used the blobby approach to combine the strictly-convex primitives of our original hyperquadric approach to achieve nonconvexity. However, given the methods introduced above, this hybrid approach is no longer necessary. The computational methods of our generalized L_p norm approach treat nonconvexity in a more consistent way and are closer to the standard polynomial constructions used in classical analytic geometry. Since any shape constructed by our methods can be substituted into the exponential forms of the usual blobby approach, we may consider these as new primitives that are elegant extensions to the forms originally considered by Blinn.

4 Examples

Our theory allows us to write down single equations for deformable shapes bounded by logical *and*'s and *or*'s of arbitrary shape primitives. Bounds corresponding to

completely arbitrary polygons, polyhedra, and D-dimensional polytopes, both connected and disconnected, can be achieved starting from shape primitives of the form of Eq. (16) containing the equations of the lines, planes, and hyperplanes of the bounding faces. The normals used for reflectance and shading calculations are computed by taking the normalized gradient of the equation at any known surface point $\vec{x}$ [5]:

$$\vec{n} = \frac{\partial F(\vec{x})}{\partial \vec{x}}. \tag{21}$$

For computer graphics purposes, such shapes can be rendered directly, by tracing a line from the camera through each pixel to the numerically-determined nearest point of the surface and computing the normal analytically to determine the pixel intensity. (Typically, one speeds up the process by using a "safe" variant of the Newton-Raphson method such as that in [10].) If the direct ray-tracing approach is unsatisfactory, a locally-faceted surface representation can be constructed using the volumetric methods of [1,7]. Or, the surface can be dynamically tesselated, with added detail in areas of high curvature. The curvature needed for this purpose can be computed analytically for any known point on the surface [5,6]. We conclude with a few simple illustrations of the method; the theoretical tools we have presented here should provide readers with ample information to devise arbitrarily complex shapes of their own.

Two Dimensions. In Figure 8, we show the deformation of an asymptotic triangle, the simplest convex shape, in four steps from a smooth blob toward its limiting boundary. Figure 9 shows the corresponding deformation of the simplest non-convex figure, an indented quadrilateral. This figure was constructed from the *and* of two half-planes intersecting at an angle with the *or* of two others, slightly displaced and meeting at a different angle.

Three Dimensions. In Figure 10, we show the deformations of a convex pentagonal wedge. Figure 11 introduces a non-convex, conical indentation made from the *or* of four half-spaces meeting at small angles, and shows several deformations.

All three-dimensional images were produced using a simple implicit function rendering algorithm we implemented on the Connection Machine[3] that assigns a processor to each pixel and passes a line through the pixel to find its nearest intersection with the surface. The two-dimensional shapes were produced in a single step by having each processor compute its local value of the implicit function in parallel.

5 Conclusion

We have proposed a generalized L_p norm in Eq. (2) as an analytic model for arbitrary shapes whose asymptotic forms as $p \to \infty$ are logical *and*'s and *or*'s of shape

[3]The Connection Machine is a registered trademark of Thinking Machines Corporation.

primitives. Shape primitives derived from linear expressions were examined in detail, since they produce asymptotic forms corresponding to arbitrary polygons and polyhedra. For special modeling purposes, any expressions whatsoever can be introduced as primitives, including recursive generalized L_p norms. Examples of shapes constructed using our approach were presented to illustrate the flexibility of the method.

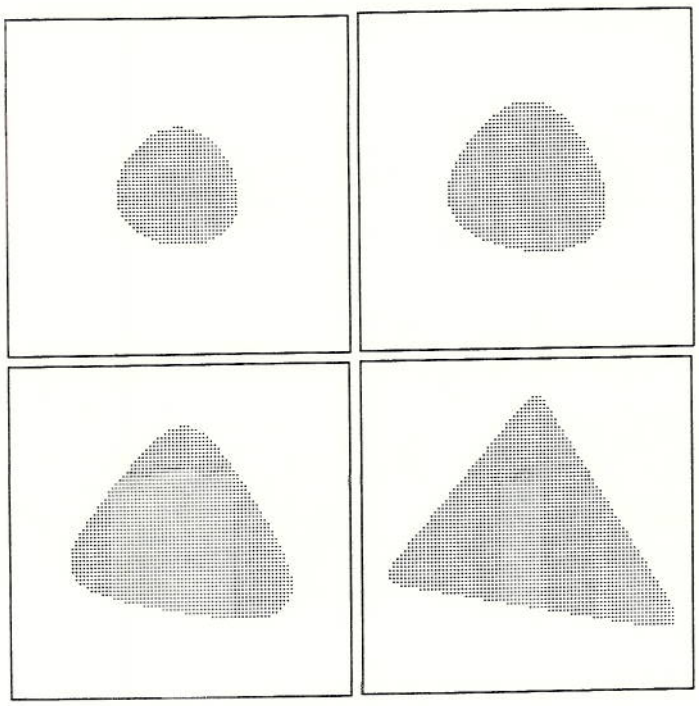

Figure 8: An asymptotic triangle constructed from the single-sided primitives and deformed towards its outer limit through exponents 0.75, 1.0, 2.0 and 10.0.

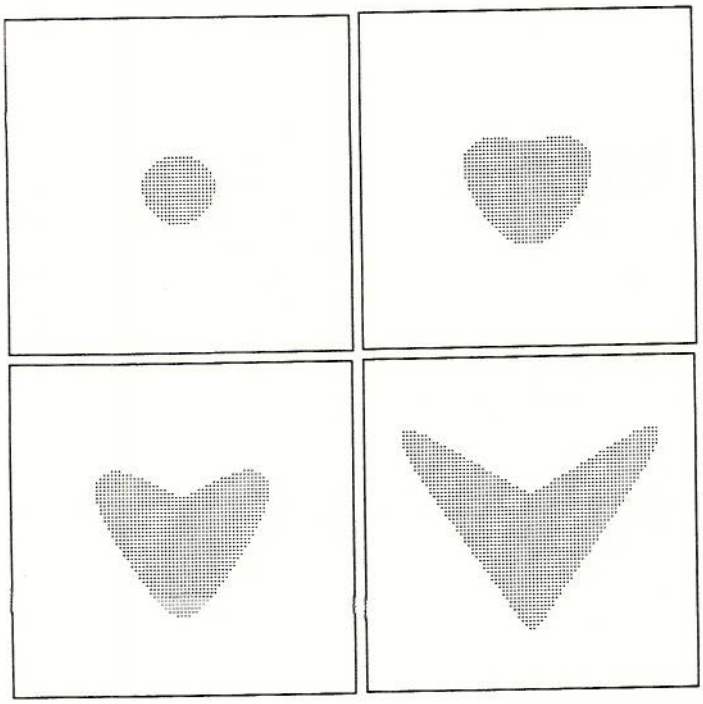

Figure 9: The simplest possible non-convex two-dimensional figure, an indented quadrilateral, constructed using the single-sided primitives. We deform it towards its asymptotic bound using exponents 0.5, 1, 2, and 10.

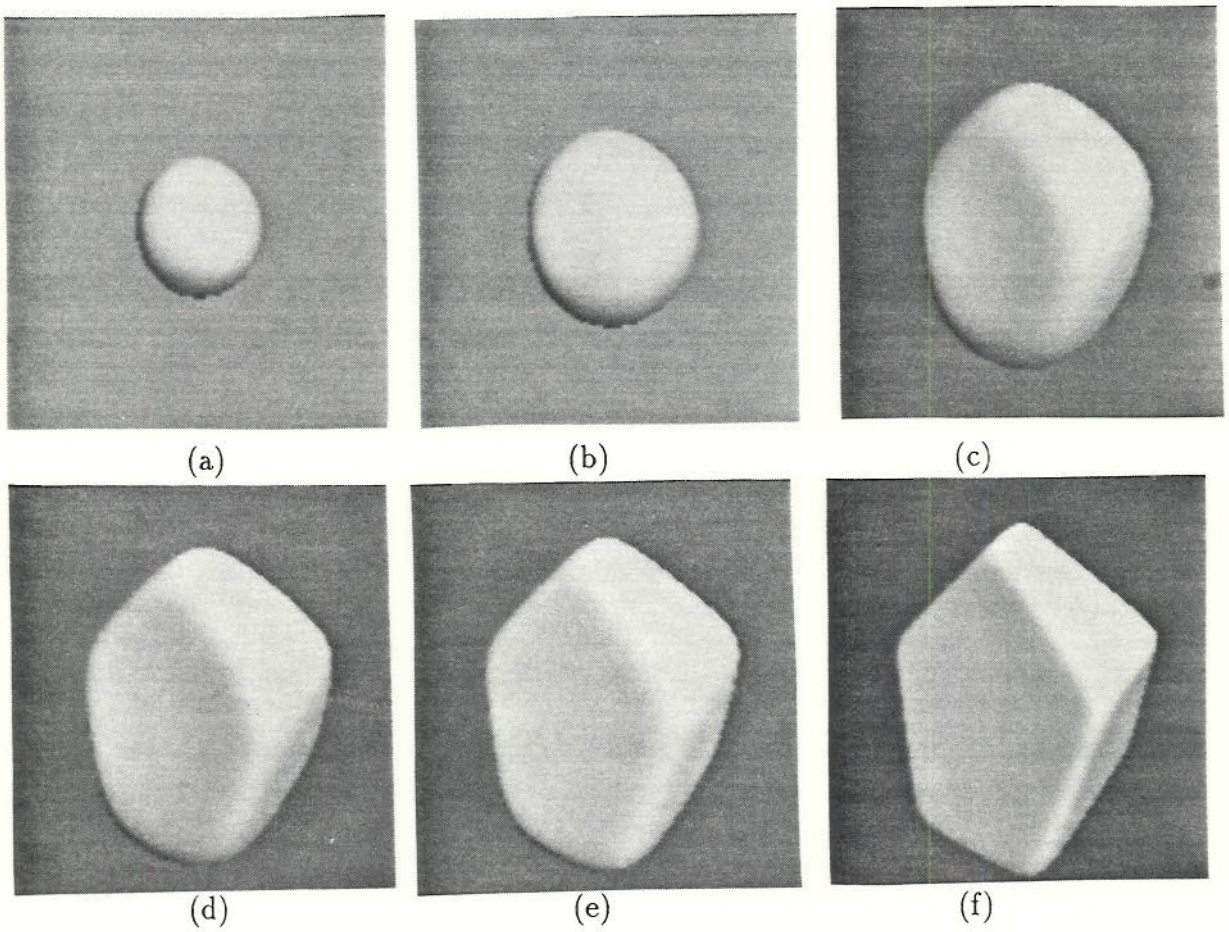

Figure 10: A convex pentagonal slab and its family of deformations.

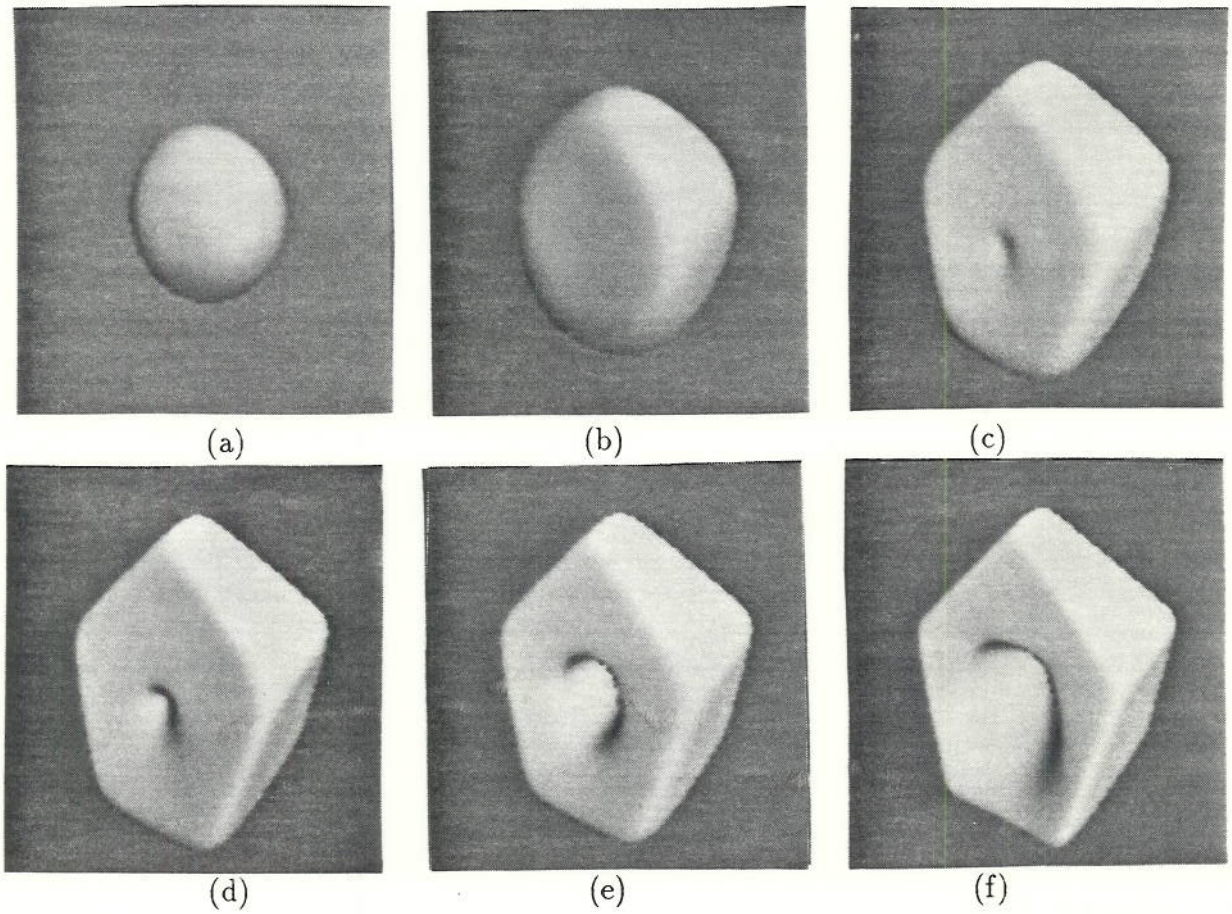

Figure 11: Deformations of a pentagonal slab combined with a nonconvex cone constructed from the *or* of four planes meeting at small angles.

References

[1] H.B. Baker, "The Weaving Wall in Tracking, Mapping and Surface Reconstruction," International Journal of Computer Vision, *in press.*

[2] A.H. Barr, Superquadrics and Angle-Preserving Transformations, *IEEE Computer Graphics and Applications* **1**, 1981, 11–23.

[3] A.H. Barr, Global and Local Deformations of Solid Primitives, *Computer Graphics* **18**, 1984, 21–30.

[4] James F. Blinn, "A Generalization of Algebraic Surface Drawing," ACM Transactions on Graphics **1**, pp. 235–256 (July 1982).

[5] L.P. Eisenhart, *A Treatise on the Differential Geometry of Curves and Surfaces,* Dover, 1960 (1909).

[6] A.J. Hanson, "Hyperquadrics: Smoothly Deformable Shapes with Convex Polyhedral Bounds," Computer Vision, Graphics and Image Processing **44**, 191–210 (1988).

[7] W.E. Lorensen and H.E. Cline, "Marching Cubes: A High Resolution 3D Surface Construction Algorithm," 1987 SIGGRAPH Proceedings, pp. 163–169.

[8] A.P. Pentland, Perceptual Organization and the Representation of Natural Form, *Artificial Intelligence* **28**, 1986, 293–331.

[9] F.P. Preparata and M.I. Shamos, *Computational Geometry — An Introduction,* (Springer-Verlag, New York, 1985); p. 216.

[10] W.H. Press, B.P. Flannery, S.A. Teukolsky, and W.T. Vetterling, *Numerical Recipes*, Cambridge University Press, 1986.